Research Square

Preprints are preliminary reports that have not undergone peer review.
They should not be considered conclusive, used to inform clinical practice,
or referenced by the media as validated information.

Graphene random spaser

Milad Sani

sani.milad@yahoo.com

Graduate University of Advanced Technology

Mahmood Hosseini Farzad

Shiraz University

Stefano Lupi

Sapienza University of Rome

Research Article

Keywords: Graphene Plasmonic, Spaser, Anderson Localization, Nano Laser

Posted Date: August 4th, 2026

DOI: https://doi.org/10.21203/rs.3.rs-10023542/v1

License: This work is licensed under a Creative Commons Attribution 4.0 International License.
Read Full License

Additional Declarations: No competing interests reported.

Version of Record: A version of this preprint was published at Plasmonics on October 10th, 2026. See the published version at https://doi.org/10.1007/s11468-026-03475-0.

Graphene random spaser

Milad Sani[1*], Mahmood Hosseini Farzad[2] and Stefano Lupi[3]

1*- Department of Fiberoptic, Institute of Science and High Technology and Environmental Sciences,

Graduate University of Advanced Technology, Kerman, Iran;

2- Department of physics, College of Science, Shiraz University, Shiraz, Iran

3-CNR-IOM and Dipartimento di Fisica, Università di Roma Sapienza, P. le Aldo Moro 2, I-00185 Roma, Italy

*Corresponding author(s). E-mail(s): sani.milad@yahoo.com;
Contributing authors; hosseinif@shirazu.ac.ir, stefano.lupi@roma1.infn.it;

Abstract

Graphene-based spasers have attracted significant interest due to the exceptional properties of monolayer graphene, including its ability to support strongly confined surface plasmons across a broad spectral range and its tunable conductivity via electrical or chemical means. In this work, we propose a novel concept of a random graphene-based spaser, consisting of a graphene monolayer deposited on a silicon–silica random grating substrate. A quantum cascade quantum well acts as the gain medium, where it is placed above the graphene layer. The inherent disorder of the substrate induces Anderson localization of the surface plasmon-polaritons (SPPs) along the graphene, enabling a fundamentally new type of nanoscale random laser which operates via the localized SPPs. Unlike conventional random lasers that rely on multiple photon scattering, the proposed random spaser operates via stimulated amplification of the localized graphene surface plasmons (GSPs), resulting in a coherent emission confined in the nano-scale range. When this structure is pumped optically above the threshold, the gain medium, non-radiatively, transfers its energy to the localized graphene surface plasmons (GSPs), producing an amplified coherent surface emission. This device functions as an efficient, compact mid-infrared nanoscale light source, with highly localized surface-bound modes. This platform paves the way for new applications in nanoscale spectroscopy, nonlinear optics, optoelectronics, and integrated photonic information processing.

Keywords: Graphene Plasmonic, Spaser, Anderson Localization, Nano Laser.

1- Introduction

Nano-optics is a branch of nanotechnology with an exponentially growing range of applications [1–7], spanning from nano-circuit devices [4] and sensors [2] to biomedicine [5] and information technology [6]. A key challenge in this field is the requirement to confine optical energy from a free-space electromagnetic beam into a sub-wavelength region to ensure compatibility with nano-optical devices.

Surface plasmon-polaritons (SPPs) at metal-dielectric interfaces enable electromagnetic energy concentration at scales of tens of nanometers, surpassing the diffraction limit [8–13]. However, ohmic losses in SPPs pose a fundamental limitation for subwavelength applications [14, 15]. Recently, this issue has been addressed by coupling surface plasmon (SP) modes with gain media [16–20]. This approach not only compensates for surface plasmon energy loss but also enables the generation of strong coherent plasmonic fields and, in certain cases, nanoscale plasmonic sources [21–23]

In this context, the spaser (surface plasmon amplification by stimulated emission of radiation) was recently introduced as the nano-plasmonic counterpart of the conventional laser [24–26]. A spaser consists of a gain medium and a plasmonic resonator arranged such that energy is transferred non-radiatively from the pumped gain medium to the plasmonic mode, thereby amplifying it [27]. The first demonstration of the spaser has been proposed by David Bergman in 2003 as coherent quantum generator of plasmonic field [28]. Since then, numerous structural designs have been developed to advance and exploit this idea. These include arrays of split-ring resonators on an active gain-medium substrate [29], a gold-film plasmonic waveguide sandwiched between two optically pumped quantum wells serving as the gain medium [30], and gold films with nano-splits surrounded by lead sulfide (PbS) quantum dots [31]. In all these structures, noble metals serve as the platform for exciting surface plasmons and a gain medium is used for compensating ohmic losses. Nevertheless, despite substantial efforts, the development of metal-based spasers remains hindered by the inherently high absorption losses of noble metals [14]. On the other hand, the unique optical and electronic properties of graphene have attracted significant research interest as an alternative platform for exciting surface plasmons [32–36]. Monolayer graphene offers outstanding electro-optical characteristics for supporting SPPs, including much lower dissipative losses compared to noble metals,

extremely strong field confinement (with a thickness under 1 nm), a wide excitation frequency range from the infrared (IR) to the terahertz (THz), relatively long SPP propagation distances, and tunable carrier density through electrostatic gating [37–41]. These features make graphene a compelling candidate for the development of graphene-based spasers.

The first graphene-based spaser was proposed theoretically by Berman et al. [42], who demonstrated that surface plasmons on an infinitely long graphene nanoribbon can be amplified by surrounding pumped quantum dots. Other approaches have also been introduced, including graphene nanoflakes coupled to optically excited carbon nanotubes [19], mid-infrared graphene spasers employing quantum cascades as the gain medium [43], and graphene plasmons embedded within a gain material [44]. Most research on graphene-based spasers has focused on closed-resonator configurations until Liu and colleagues introduced the first graphene-based spaser employing an open resonator [45].

Such an open-cavity spaser can function as a coherent plasmon source, a highly efficient sensor, and an integrated component for ultrafast, subwavelength nano-circuit applications [14,46,47]. Motivated by these advances, we have recently studied the effect of Anderson localization on the excitation and propagation of surface plasmons in monolayer graphene [48,49]. As noted, a spaser is the plasmonic counterpart of a laser, enabling coherent surface plasmon emission. In this work, we propose a novel spaser called the "random spaser"—the first demonstration analogous to a random laser. Our design uses an open resonator under Anderson localization, formed by placing a graphene monolayer on a random silicon-silica grating. This grating creates spatial disorder in graphene's effective refractive index, localizing surface plasmons along their propagation path due to the Anderson localization effect. Additionally, a quantum cascade structure is integrated above the graphene layer to amplify the randomly localized graphene surface-plasmon (GSP) modes. This configuration serves as a source of amplified surface plasmons under Anderson localization conditions.

We believe this work opens a new avenue for fabricating spasers with random structural features, random spasers, providing a source of highly localized surface plasmon polaritons (SPPs) on monolayer graphene. Similar to the role of random lasers in advancing conventional laser science, the concept of the random spaser may inspire new developments in nanofabrication and plasmonic device applications. This article is organized as follows: first, we describe the structure of the proposed graphene-based spaser. Next, we introduce the gain medium used in the random spaser. Subsequent sections present a two-dimensional simulation analysis of the random spaser's performance, focusing on the interaction between localized graphene surface plasmons and the gain medium. Finally, the article concludes with a summary of the key findings.

2- Methods

The proposed random spaser is realized by placing a graphene monolayer atop a silicon–silica random grating, with a quantum cascade well (QCW) layer positioned above the graphene (Fig. 1).

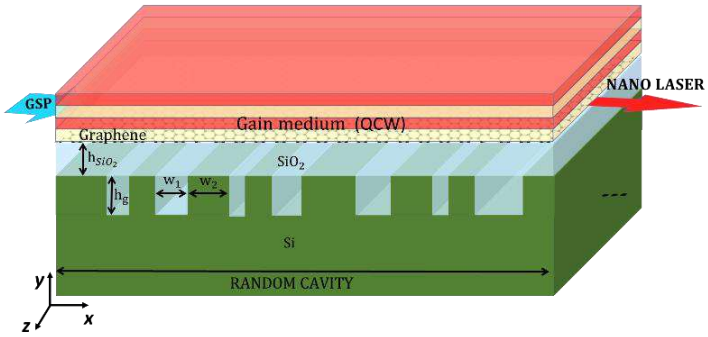


FIG. 1. Schematic illustration of graphene random spaser structure with randomness (δ) of 20% in graphene substrate. The blue arrow (from the left side) shows the propagating graphene surface plasmon. The silicon substrate (green color) features a groove grating structure with a depth of hg and a width of w2. hSiO2 denotes the distance between the graphene and Si substrate, which is a silica layer and is shown by blue color. The gain medium is the quantum cascade well, which is observed by yellow and red colors. The red arrow on the right side shows the spaser output, which in turn can be coupled to another nanoscale optic structure.

The random grating serves as a refractive index modulator for the graphene, while the QCW functions as the gain medium of the spaser. As shown in Fig. 1, the widths of the grating trenches and ridges change the optical conductivity of the monolayer graphene and therefore its refractive index. This causes the surface plasmons to interact at the same time with both the disordered graphene and the gain medium.

A. Modulated monolayer graphene

As previously noted, graphene's exceptional properties position it as a superior alternative to noble metals in plasmonic structures [39,42,44,50]. Notably, its high carrier concentration and mobility substantially extend the propagation length of surface plasmon polaritons (SPPs) on monolayer graphene, rendering it highly suitable for open-resonator spaser

applications. The graphene layer is modulated via its frequency-dependent optical conductivity, expressed as the sum of interband and intraband contributions [51].

$$\sigma_g(\omega) = \frac{ie^2 k_B T}{\pi\hbar^2(\omega+i\tau^{-1})}\left[\frac{\mu_c}{k_B T} + 2\ln\left[\exp\left(-\frac{\mu_c}{k_B T}+1\right)\right]\right] + \frac{ie^2}{4\pi\hbar}\ln\left[\frac{2|\mu_c|-\hbar(\omega+i\tau^{-1})}{2|\mu_c|+\hbar(\omega+i\tau^{-1})}\right] \quad (1)$$

Here, e, ω and k_B are the charge of electron, photon frequency in vacuum and Boltzmann constant, respectively. The temperature T is assumed about room temperature, i.e., T = 300K. In addition, the momentum relaxation time τ is related to chemical potential μ_c and carrier mobility μ via $\tau = \mu\mu_c/(e\nu_f)^2$, where $\nu_f = 10^6$m/s is the fermi velocity. The carrier mobility μ is experimentally estimated to be μ = 20000 $cm^2V^{-1}s^{-1}$ at room temperature [52–54]. The chemical potential plays the main role in modulation of graphene, since it can be expressed a $\mu_c = k\nu_f(\pi n)^{1/2}$ and can be tuned by controlling doping density n, which is related to the electric potential difference V and material and height of substrate via $n = \epsilon_d\epsilon_0 V/eH$. Here, ϵ_d and ϵ_0 are the relative permitivities of substrate (in this case SiO_2) and free space, respectively. H is the height of silica below graphene layer, which can effectively be used to control $\sigma_g(\omega)$ and, consequently, modulate the refractive index of graphene monolayer. In the proposed structure, H alternates between h_{SiO_2} and $h_g + h_{SiO_2}$ providing two different refractive indices n_{eff1} and n_{eff2} on the graphene layer in a periodic or random manner. Under the periodic variation of these refractive indices the graphene layer behaves like a Bragg grating for GSP waves propagates on it, of course the condition

$$w_1 n_{eff_1} + w_2 n_{eff_2} = m\lambda_b \quad (2)$$

Must be satisfied. where, w_1 and w_2 are widths of trenches and ridges, respectively and λ_b is Bragg wavelength.
When the frequencies of GSP modes are below the optical phonon frequency of monolayer graphene, the damping of GSP modes due to the interaction of oscillating electrons with optical phonons is insignificant [52, 55]. In the proposed structure, the geometrical parameters (i.e., h_g, h_{SiO}, w_1 and w_2) are adjusted in such a way that the graphene monolayer becomes eligible for supporting GSP modes at midinfrared frequency band, which is apparently below the optical phonon frequency of monolayer graphene (≈ 1600 cm^{-1}). In this regard, these parameters are set as $w_1 = w_1$=40nm, $\mathbf{h_g} = \mathbf{h_{SiO_2}}$ = 40nm, which results in equally spaced square ridges and trenches.

B. Randomness

The occurrence of Anderson localization of graphene surface-plasmon (GSP) modes on a randomly modulated graphene monolayer has been demonstrated in previous works [48,49]. These localized modes offer strong potential for interaction with the gain medium, which in turn can lead to significant amplification of GSPs. In the proposed structure, randomness is introduced by adding a disorder term, δwi (i = 1, 2), to the widths of the grating trenches and ridges, such that $w_i = w_i + \delta w_i$. Numerically, this disorder is generated as $\delta w_i = \alpha \times u \times w_i$, where $u$is a random number uniformly distributed between –1 and 1, and $\alpha$is the randomness factor. For example, with $w_1 = w_2 = 40$nm and $\alpha = 0.1$, the widths of the trenches and ridges vary randomly between 36 and 44 nm.

C. Quantum cascade gain medium

In any spaser structure, a gain medium is employed to compensate for losses and reinforce the surface plasmon polaritons (SPPs). Practically, several candidates exist for this role, including quantum cascade gain media [43,56], nonlinear media for frequency mixing [57], and optically pumped carbon nanotubes acting as semiconductors [19]. Considering the strong confinement of graphene surface-plasmon (GSP) modes in the normal (y) direction on the graphene layer (Fig. 1), a quantum cascade well (QCW) is the preferred gain medium for the proposed random spaser, as it can efficiently interact with the confined field [43]. Furthermore, the gain spectrum of a QCW can be readily tuned by adjusting the thickness of its constituent layers, since it is fundamentally determined by quantum confinement effects. Additionally, the excellent thermal stability and the capability of electrical pumping make QCWs a highly suitable choice for the proposed spaser.

The pump energy stored in the QCW medium is transferred non-radiatively to the GSP modes. As the GSP modes are amplified, the rate of this non-radiative decay increases, which reduces the population inversion in the gain medium and leads to gain saturation. Neglecting this saturation in numerical simulations can result in unphysical outcomes due to unlimited mode amplification. Accordingly, the gain of the QCW, γ, as a function of frequency $\omega$and pump power p, can be expressed as

$$\gamma = \frac{\gamma_0(\omega)}{1+\frac{p_{sp}^2}{p_{sat}^2}} \quad (3)$$

where $\gamma_0(\omega, p)$ is small signal gain of the quantum cascade which has a direct relationship with p. Moreover, p_{sp} and p_{sat} are the power of GSP modes and saturation power of the gain medium, respectively. Consequently, the gain can be incorporated into numerical method via negative conductivity, as

$$\sigma = \frac{\sigma_0(\omega)}{1+\frac{p_{sp}^2}{p_{sat}^2}} \quad (4)$$

where σ_0 is the conductivity associated to the small signal gain and its frequency dependency can be obtained from the fluorescence curve of gain medium (QCW).

The nonlinear finite element method has been used for analyzing the proposed random spaser to handle the nonlinear conductivity of the gain medium. The numerical simulation is repeatedly applied for wavelength steps in the rage (5.9µm−6.2µm) and the steady state results are gathered to cover the full frequency span.

3- Analysis of random spaser performance

First, the perfectly ordered case (α = 0) which is a periodically modulated graphene without any amplification (pump power p = 0), is investigated. As shown in Figure (1), the incident wave excites the GSP modes on the excitation region and the transmission is detected at the end of the spaser region. While the GSP modes are propagating through this induced periodic variation of effective refractive index on the graphene monolayer, several partial reflections and transmissions occur.

Constructive and destructive interference of these waves leads to the appearance of passband and stopband in the transmission spectrum of the structure. As illustrated in Fig. 2a, the stopband occurs in the wavelength range λ = 6.24 μm to λ = 6.38 μm. The central wavelength of the stopband, which is approximately 6.28 μm, can be determined from the Bragg condition (Eq. 2). The behavior of GSP modes with the passband or stopband frequencies can be realized from the 3D plot of Fig. 2b, which shows the spatial and spectral distribution of GSP modes, simultaneously. It can be seen that, at the stopband, the GSPs rapidly decay after a few tens of nanometers, and unlike the passband modes, the stopband modes cannot survive to the end of the structure.

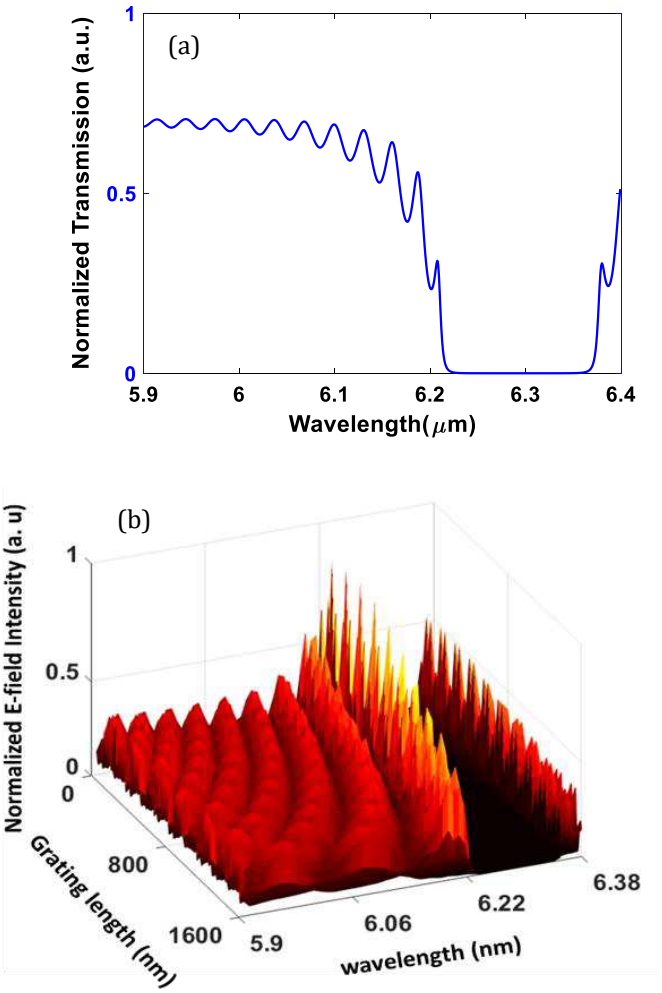


Figure. 2: (a) Transmission spectrum for SPs on monolayer graphene which lay on the periodic silicon-silica grating (like a photonic crystal). (b) Normalized transmitted field intensity distribution ($|E_x|^2/|E_0|^2$) (Ex is the corresponding electric field along the propagation direction x and E_0 is the maximum value of E_x for periodic grating) as a function of wavelength and the position on the graphene, under the same situation as the part (a).

When the randomness factor increases, the randomly modulated graphene layer produces partially reflected or transmitted GSPs with random amplitudes and phases. It was previously demonstrated that the interference of these waves leads to occurrence of Anderson localized modes [48, 49]. In the proposed structure, the Anderson localization of GSPs results in the appearance of narrow peaks in the transmission spectrum which is illustrated in Fig. 3a for α = 0.2. It can be seen that the passband is divided into sharp peaks with high quality factors. For instance, the Q-factor of the peak at 6.18 µm is estimated to be greater than 250. The origin of these peaks is revealed in Fig. 3b which shows the spatial and spectral distribution of the modes. It can be observed that, the peaks of Fig. 3a and the localized modes of Fig. 3b take place at the same wavelengths. In other words, the leakage of localized modes forms the peaks of the transmission spectrum.

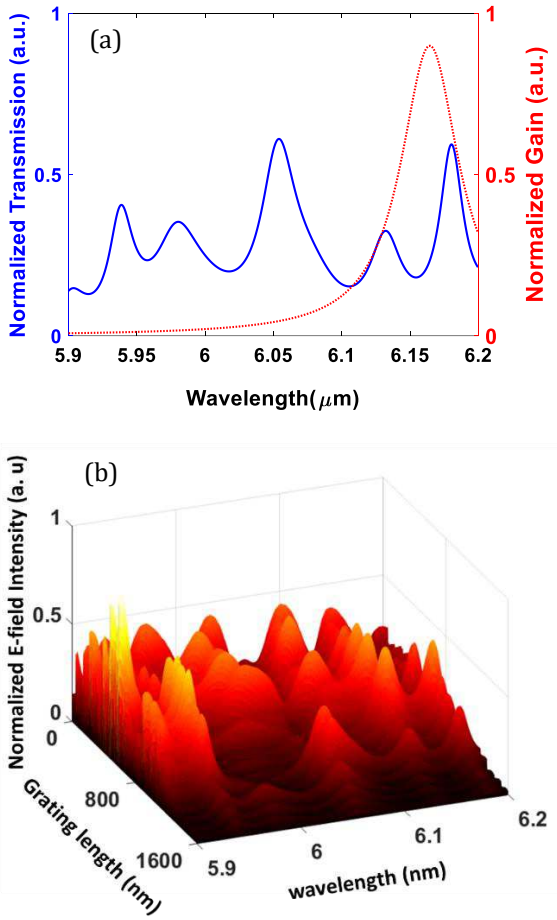


Figure. 3: (a) Transmission spectrum of graphene based random grating for for the δ=20% and g<g_{th}. The dashed line (red color in online print) in this figure shows the normalized gain spectrum of quantum cascade medium. (b) The normalized field intensity distribution $|E_x|^2/|E_0|^2$ (here E_0 is the maximum value of E_x for periodic grating) as a function of wavelength and the position on the graphene for the δ=20% and g<g_{th}.

To provide a better understanding, the gain spectrum is also plotted in Fig. 3a (red broken line). The sharp narrow peaks with high Q-factor under the gain curve show at potential for being the main mode of the spaser. So, they can be called quasi-modes of the spaser. There are two important parameters that determine which quasi- mode wins the competition to be the main mode of the spaser: (i) Q-factor; i.e., the quasi mode with higher Q- factor has the lowest loss so it can start spasing with smaller gain threshold. (ii) Spectral position of quasi mode; i.e., the quasi-mode with closest wavelength to the maximum of the gain spectrum has more chance to increasingly catch energy from the gain medium and be- come the main mode of the spaser.

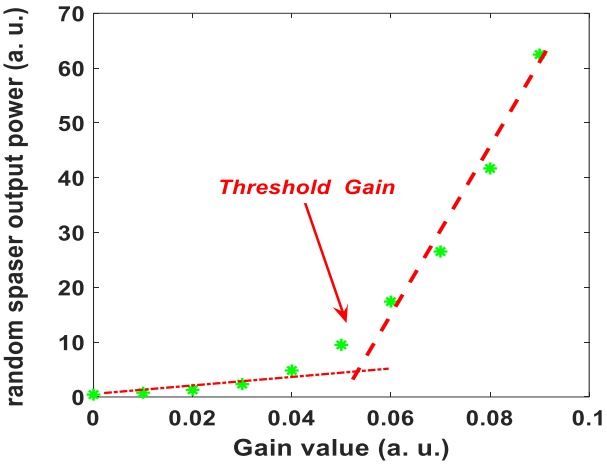


Figure. 4: The output power of random spaser at 6.82 µm by increasing the gain value. Data evolution vs. gain (green points) are described with two red dashed lines. The threshold value is estimated through the intersection of the two lines.

According to the above discussion, for the current configuration, the quasi-mode at λ = 6.18 μm has the highest likelihood of becoming the main spasing mode. Figure 4 shows how the output power of this quasi-mode varies with increasing gain. Initially, the output power rises slowly with gain, followed by a rapid increase once the gain

exceeds a threshold value. To highlight these trends, two dashed lines are fitted to the data as a guide to the eye. The threshold gain, g_{th}, can be estimated from the intersection of these lines. At this threshold, the gain of the QCW medium exactly compensates for the losses of the propagating GSPs. Above the threshold, the energy transferred from the gain medium to the Anderson-localized modes exceeds the losses, leading to a significant increase in output power.

It should be noted that the behavior observed in Figure. 4 reflects an important characteristic of all laser and spasers [58,59]. The threshold gain in the proposed disordered structure is expected to be lower than that in a periodic structure. Indeed, the spaser modes in our disordered structure arise from Anderson localization, exhibiting a quality factor higher than that of GSP modes in a periodic structure [53].

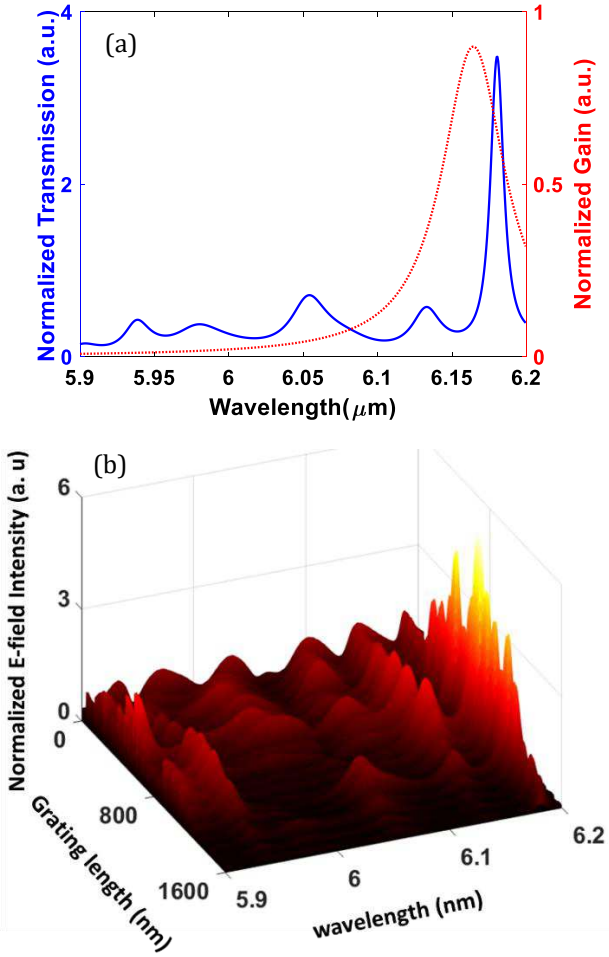


Figure. 5: (a) Transmission spectrum of graphene based random grating for for the δ=20% and g=1.2g_{th}. The dashed line (red color in online print) in this figure shows the normalized gain spectrum of quantum cascade medium. (b) The normalized field intensity distribution $|E_x|^2/|E_0|^2$ (here E_0 is the maximum value of E_x for periodic grating) as a function of wavelength and the position on the graphene for the δ=20% and g=1.2g_{th}.

It can be seen from the above analysis that the proposed graphene-based random structure operates as a spaser, producing stimulated surface plasmons. It is, however, important to examine the coherence and single-mode behavior of this spaser. Figure 5a shows the transmission spectrum of the structure for $\alpha = 0.2$and $g = 1.2\ g_{th}$. As the gain increases, only one of the quasi-modes from Figure 3a (the peak at 6.18 μm) evolves into the spaser mode. The spatial and spectral distribution of the localized modes is shown in Figure 5b. While many highly localized modes with narrow wavelength widths exist across the graphene layer, only one successfully absorbs energy and is significantly amplified.

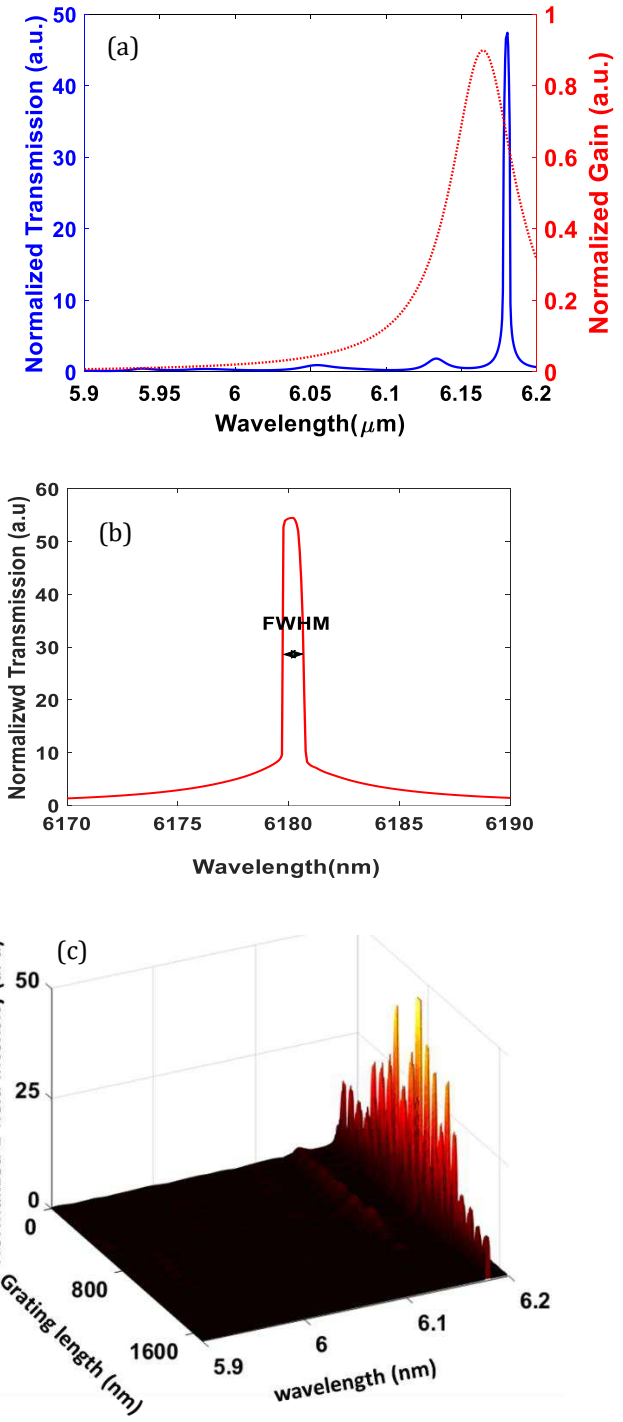


Figure. 6: (a) Transmission spectrum of graphene based random grating for δ=20% and g=4g_{th}. The dashed line (red color in online print) in this figure shows the normalized gain spectrum of quantum cascade medium. (b) Transmission spectrum of the spaser mode for δ=20% and g=4g_{th} . (c) The normalized field intensity distribution $|E_x|^2/|E_0|^2$ (here E_0 is the maximum value of E_x for periodic grating) as a function of wavelength and the position on the graphene for the δ=20% and g=4g_{th}.

To investigate the coherence of the spaser, the full-width at half-maximum (FWHM) of the output provides a useful measure. Figure 6a shows the transmission spectrum for $\alpha = 0.2$ and $g = 4\ g_{\text{th}}$. The FWHM of the dominant spaser mode (Figure 6b) is estimated to be approximately 1.1 nm, indicating a satisfactory level of coherence. This can also be expressed in terms of the coherence length, $l_c = \lambda^2/2\Delta\lambda$, which is calculated to be around 1.1 μm for the current case.

The spatial and spectral distribution of GSPs is shown in Figure 6c, clearly highlighting the dominance of the main spaser mode. For a more comprehensive understanding of the spaser's operation, the side-view of the electric field distribution over the x–y plane is presented in Figure 7 for two cases: (a) $\alpha = 0.2$and $g = 0$, corresponding to Figure 3, and (b) $\alpha = 0.2$and $g = 4\ g_{\text{th}}$, corresponding to Figure 6. Comparing these cases, it is evident that the gain medium dramatically enhances the localized GSP modes when the gain significantly exceeds the threshold.

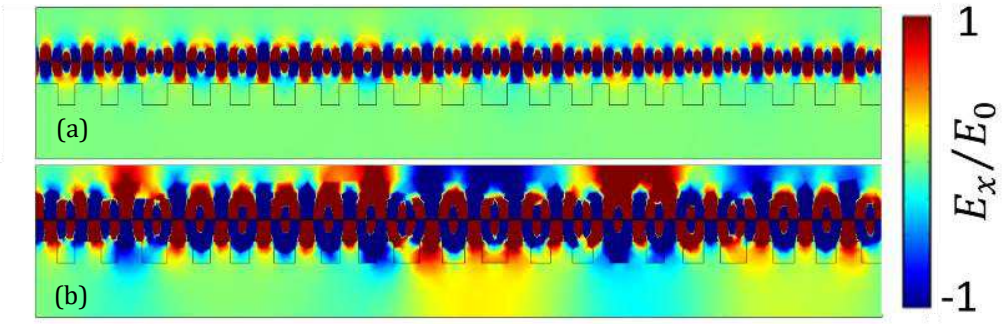


Figure 7. The side-view of E_x-field intensity distribution along the graphene layer in x-y plane (see figure 1) for (a) propagated GSP with the gain value below the threshold value at 6.82 µm and (b) excited GSP with the gain value above the threshold gain ($g=4g_{th}$) at 6.82 µm.

As mentioned earlier, the GSPs are localized within local cavities along the graphene layer. To examine how optical amplification affects these cavities, the electric field distribution is analyzed in two scenarios: without gain ($g = 0$) and with gain ($g = 4\ g_{\text{th}}$).

Figure 8a shows the side-view electric field distribution for the case without amplification. Here, the highest intensity is localized in a cavity positioned around 900 nm. When the gain is increased to $4\ g_{\text{th}}$(Figure 8b), the spatial position of the cavity remains unchanged, but the localized intensity within it is amplified by a factor of 60. This comparison confirms that the random spaser consists of multiple spatially random cavities, which generate the random spaser output in a manner similar to conventional random lasers.

Based on the above discussions, the proposed structure can serve as a high-performance random spaser. Its output acts as a source of amplified surface plasmons in the presence of Anderson localization. This excited electric field at the nanoscale can be coupled to other nanostructures for a variety of applications, including nanosensors, nanospectroscopy, nonlinear optics, and optoelectronics, opening new avenues for the design and fabrication of conventional spasers.

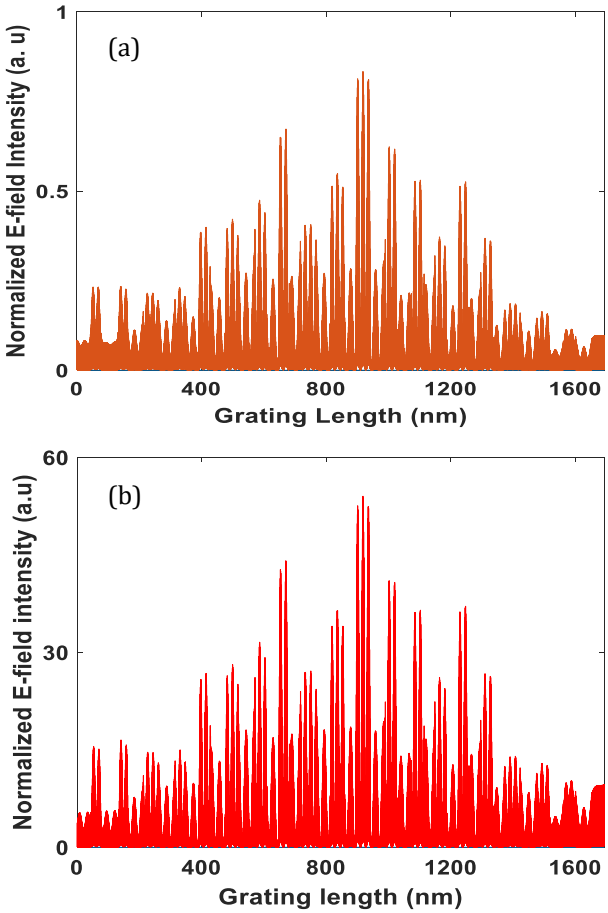


Figure 8. The E_x-field intensity distribution on the graphene layer (see figure 1) for (a) propagated GSP with the gain value below the threshold value at 6.18 µm and (b) excited GSP with the gain value above the threshold gain ($g=4g_{th}$) at 6.18 µm.

4- conclusion

In conclusion, we have proposed a novel graphene-based random spaser that exploits the unique plasmonic properties of monolayer graphene and the Anderson localization of surface plasmon-polaritons (SPPs) induced by a silicon–silica random grating substrate. By incorporating a quantum cascade well as a gain medium positioned above the graphene layer, we have shown that localized graphene surface plasmon modes can be efficiently amplified beyond the lasing threshold, leading to a coherent mid-infrared emission with strong spatial confinement.

This work extends the concept of random lasers into the plasmonic domain, introducing a new class of nanoscale coherent light sources. The proposed random spaser offers a compact, tunable, and efficient platform with promising applications in nanoscale spectroscopy, nonlinear optics, optoelectronics, and integrated photonic information processing. These findings establish a foundation for the future experimental realizations and open up new avenues for the development of advanced plasmonic nanolasers.

Declarations

Author Contributions Three authors worked on the concept.

Funding Not applicable.

Availability of data and material The datasets generated during and/or analyzed during the current study are available from the corresponding author on reasonable request.

Ethics Approval Not applicable.

Consent to Participate Not applicable.

Consent for Publication Three authors consent to publication.

Conflict of Interest The authors have no conflicts of interest to declare that are relevant to the content of this article.

References

1. Juan, M. L.; Righini, M.; Quidant, R., Plasmon nano-optical tweezers. *Nature Photonics* **2011,** *5* (6), 349-356.
2. Lal, S.; Link, S.; Halas, N. J., Nano-optics from sensing to waveguiding. *Nature Photonics* **2007,** *1* (11), 641-648.
3. Bouhelier, A.; Renger, J.; Beversluis, M. R.; Novotny, L., Plasmon-coupled tip-enhanced near-field optical microscopy. *Journal of Microscopy* **2003,** *210* (3), 220-224.
4. Bozhevolnyi, S. I. In *Plasmonic Nano-Guides and Circuits*, Frontiers in Optics 2008/Laser Science XXIV/Plasmonics and Metamaterials/Optical Fabrication and Testing, Rochester, New York, 2008/10/19; Optical Society of America: Rochester, New York, 2008; p MWD3.
5. Shi, X.; Gong, H.; Li, Y.; Wang, C.; Cheng, L.; Liu, Z., Graphene-based magnetic plasmonic nanocomposite for dual bioimaging and photothermal therapy. *Biomaterials* **2013,** *34* (20), 4786-4793.
6. Merlo, J. M.; Nesbitt, N. T.; Calm, Y. M.; Rose, A. H.; D'Imperio, L.; Yang, C.; Naughton, J. R.; Burns, M. J.; Kempa, K.; Naughton, M. J., Wireless communication system via nanoscale plasmonic antennas. *Scientific Reports* **2016,** *6*, 31710.

7. Khaliji, K.; Biswas, S. R.; Hu, H.; Yang, X.; Dai, Q.; Oh, S.-H.; Avouris, P.; Low, T., Plasmonic Gas Sensing with Graphene Nanoribbons. *Physical Review Applied* **2020,** *13* (1), 011002.

8. Kravets, V. G.; Kabashin, A. V.; Barnes, W. L.; Grigorenko, A. N., Plasmonic Surface Lattice Resonances: A Review of Properties and Applications. *Chemical Reviews* **2018,** *118* (12), 5912-5951.

9. Yeshchenko, O. A.; Kozachenko, V. V.; Tomchuk, A. V.; Haftel, M.; Knize, R. J.; Pinchuk, A. O., Plasmonic Metasurfaces with Tunable Gap and Collective Surface Plasmon Resonance Modes. *The Journal of Physical Chemistry C* **2019,** *123* (20), 13057-13062.

10. Yu, H.; Peng, Y.; Yang, Y.; Li, Z.-Y., Plasmon-enhanced light–matter interactions and applications. *npj Computational Materials* **2019,** *5* (1), 45.

11. Christensen, J.; Manjavacas, A.; Thongrattanasiri, S.; Koppens, F. H. L.; García de Abajo, F. J., Graphene Plasmon Waveguiding and Hybridization in Individual and Paired Nanoribbons. *ACS Nano* **2012,** *6* (1), 431-440.

12. D'apuzzo, F.; Esposito, M.; Cuscunà, M.; Cannavale, A.; Gambino, S.; Lio, G. E.; De Luca, A.; Gigli, G.; Lupi, S., Mid-Infrared Plasmonic Excitation in Indium Tin Oxide Microhole Arrays. *ACS Photonics* **2018,** *5* (6), 2431-2436.

13. Limaj, O.; D'Apuzzo, F.; Di Gaspare, A.; Giliberti, V.; Domenici, F.; Sennato, S.; Bordi, F.; Lupi, S.; Ortolani, M., Mid-Infrared Surface Plasmon Polariton Sensors Resonant with the Vibrational Modes of Phospholipid Layers. *The Journal of Physical Chemistry C* **2013,** *117* (37), 19119-19126.

14. Azzam, S. I.; Kildishev, A. V.; Ma, R.-M.; Ning, C.-Z.; Oulton, R.; Shalaev, V. M.; Stockman, M. I.; Xu, J.-L.; Zhang, X., Ten years of spasers and plasmonic nanolasers. *Light: Science & Applications* **2020,** *9* (1), 90.

15. Ramezani, M.; Halpin, A.; Fernández-Domínguez, A. I.; Feist, J.; Rodriguez, S. R.-K.; Garcia-Vidal, F. J.; Gómez Rivas, J., Plasmon-exciton-polariton lasing. *Optica* **2017,** *4* (1), 31-37.

16. Shahbazyan, T. V., Mode Volume, Energy Transfer, and Spaser Threshold in Plasmonic Systems with Gain. *ACS Photonics* **2017,** *4* (4), 1003-1008.

17. Passarelli, N.; Bustos-Marún, R. A.; Coronado, E. A., Spaser and Optical Amplification Conditions in Gold-Coated Active Nanoparticles. *The Journal of Physical Chemistry C* **2016,** *120* (43), 24941-24949.

18. Wang, J.-H.; Gao, Z.; Song, P.; Melentiev, P. N.; Wang, X.-H.; Gao, H.; Yang, F.; Kang, B.; Xu, J.-J.; Chen, H.-Y., How Gain Layer Design Determines Performance of Nanoparticle-Based Spaser. *The Journal of Physical Chemistry C* **2020,** *124* (30), 16553-16560.

19. Rupasinghe, C.; Rukhlenko, I. D.; Premaratne, M., Spaser Made of Graphene and Carbon Nanotubes. *ACS Nano* **2014,** *8* (3), 2431-2438.

20. Ma, R.-M.; Oulton, R. F.; Sorger, V. J.; Bartal, G.; Zhang, X., Room-temperature sub-diffraction-limited plasmon laser by total internal reflection. *Nature Materials* **2011,** *10* (2), 110-113.

21. Oulton, R. F.; Sorger, V. J.; Zentgraf, T.; Ma, R.-M.; Gladden, C.; Dai, L.; Bartal, G.; Zhang, X., Plasmon lasers at deep subwavelength scale. *Nature* **2009,** *461* (7264), 629-632.

22. Noginov, M. A.; Zhu, G.; Belgrave, A. M.; Bakker, R.; Shalaev, V. M.; Narimanov, E. E.; Stout, S.; Herz, E.; Suteewong, T.; Wiesner, U., Demonstration of a spaser-based nanolaser. *Nature* **2009,** *460* (7259), 1110-1112.

23. Hill, M. T.; Marell, M.; Leong, E. S. P.; Smalbrugge, B.; Zhu, Y.; Sun, M.; van Veldhoven, P. J.; Geluk, E. J.; Karouta, F.; Oei, Y.-S.; Nötzel, R.; Ning, C.-Z.; Smit, M. K., Lasing in metal-insulator-metal sub-wavelength plasmonic waveguides. *Opt. Express* **2009,** *17* (13), 11107-11112.

24. Chou, Y.-H.; Hong, K.-B.; Chang, C.-T.; Chang, T.-C.; Huang, Z.-T.; Cheng, P.-J.; Yang, J.-H.; Lin, M.-H.; Lin, T.-R.; Chen, K.-P.; Gwo, S.; Lu, T.-C., Ultracompact Pseudowedge Plasmonic Lasers and Laser Arrays. *Nano Letters* **2018,** *18* (2), 747-753.

25. Koenderink, A. F., Plasmon Nanocavity Array Lasers: Cooperating over Losses and Competing for Gain. *ACS Nano* **2019,** *13* (7), 7377-7382.

26. Li, H.; Li, J.-H.; Hong, K.-B.; Yu, M.-W.; Chung, Y.-C.; Hsu, C.-Y.; Yang, J.-H.; Cheng, C.-W.; Huang, Z.-T.; Chen, K.-P.; Lin, T.-R.; Gwo, S.; Lu, T.-C., Plasmonic Nanolasers Enhanced by Hybrid Graphene–Insulator–Metal Structures. *Nano Letters* **2019,** *19* (8), 5017-5024.

27. Zhang, Q.; Li, G.; Liu, X.; Qian, F.; Li, Y.; Sum, T. C.; Lieber, C. M.; Xiong, Q., A room temperature low-threshold ultraviolet plasmonic nanolaser. *Nature Communications* **2014,** *5* (1), 4953.

28. Bergman, D. J.; Stockman, M. I., Surface Plasmon Amplification by Stimulated Emission of Radiation: Quantum Generation of Coherent Surface Plasmons in Nanosystems. *Physical Review Letters* **2003,** *90* (2), 027402.

29. Zheludev, N. I.; Prosvirnin, S. L.; Papasimakis, N.; Fedotov, V. A., Lasing spaser. *Nature Photonics* **2008,** *2* (6), 351-354.

30. Flynn, R. A.; Kim, C. S.; Vurgaftman, I.; Kim, M.; Meyer, J. R.; Mäkinen, A. J.; Bussmann, K.; Cheng, L.; Choa, F. S.; Long, J. P., A room-temperature semiconductor spaser operating near 1.5 μm. *Opt. Express* **2011,** *19* (9), 8954-8961.

31. Plum, E.; Fedotov, V. A.; Kuo, P.; Tsai, D. P.; Zheludev, N. I., Towards the lasing spaser: controlling metamaterial optical response with semiconductor quantum dots. *Opt. Express* **2009,** *17* (10), 8548-8551.

32. Low, T.; Avouris, P., Graphene Plasmonics for Terahertz to Mid-Infrared Applications. *ACS Nano* **2014,** *8* (2), 1086-1101.

33. Hong, H. Y.; Ha, J. S.; Lee, S.-S.; Park, J. H., Effective Propagation of Surface Plasmon Polaritons on Graphene-Protected Single-Crystalline Silver Films. *ACS Applied Materials & Interfaces* **2017,** *9* (5), 5014-5022.

34. Desouky, M.; Anisur, M. R.; Alba, M.; Raman, R. K. S.; Swillam, M. A.; Voelcker, N. H.; Kasry, A., Near-Field Mapping of Localized Plasmon Resonances in Metal-Free, Nanomembrane Graphene for Mid-Infrared Sensing Applications. *ACS Applied Nano Materials* **2018,** *1* (11), 6454-6462.

35. D'Apuzzo, F.; Piacenti, A. R.; Giorgianni, F.; Autore, M.; Guidi, M. C.; Marcelli, A.; Schade, U.; Ito, Y.; Chen, M.; Lupi, S., Terahertz and mid-infrared plasmons in three-dimensional nanoporous graphene. *Nature Communications* **2017,** *8* (1), 14885.

36. Yang, H.; Jin, X.; Sun, G.; Li, Z.; Gao, J.; Lu, B.; Shao, C.; Zhang, X.; Dai, C.; Zhang, Z.; Chen, N.; Lupi, S.; Marcelli, A.; Qu, L., Retarding Ostwald Ripening to Directly Cast 3D Porous Graphene Oxide Bulks at Open Ambient Conditions. *ACS Nano* **2020,** *14* (5), 6249-6257.

37. Lozovik, Y. E., Plasmonics and magnetoplasmonics based on graphene and a topological insulator. *Physics-Uspekhi* **2012,** *55* (10), 1035-1039.

38. Mikhailov, S. A., Graphene-based voltage-tunable coherent terahertz emitter. *Physical Review B* **2013,** *87* (11), 115405.

39. Grigorenko, A. N.; Polini, M.; Novoselov, K. S., Graphene plasmonics. *Nature Photonics* **2012,** *6*, 749.

40. Hwang, E. H.; Das Sarma, S., Dielectric function, screening, and plasmons in two-dimensional graphene. *Physical Review B* **2007,** *75* (20), 205418.

41. Qian, H.; Ma, Y.; Yang, Q.; Chen, B.; Liu, Y.; Guo, X.; Lin, S.; Ruan, J.; Liu, X.; Tong, L.; Wang, Z. L., Electrical Tuning of Surface Plasmon Polariton Propagation in Graphene–Nanowire Hybrid Structure. *ACS Nano* **2014,** *8* (3), 2584-2589.

42. Berman, O. L.; Kezerashvili, R. Y.; Lozovik, Y. E., Graphene nanoribbon based spaser. *Physical Review B* **2013,** *88* (23), 235424.

43. Apalkov, V.; Stockman, M. I., Proposed graphene nanospaser. *Light: Science &Amp; Applications* **2014,** *3*, e191.

44. Altares Menendez, G.; Rosolen, G.; Maes, B., Graphene plasmons embedded in a gain medium: layer and ribbon plasmons. *Journal of Optics* **2016,** *18* (12), 125004.

45. Liu, B.; Zhu, W.; Gunapala, S. D.; Stockman, M. I.; Premaratne, M., Open Resonator Electric Spaser. *ACS Nano* **2017,** *11* (12), 12573-12582.

46. Ma, R.-M.; Ota, S.; Li, Y.; Yang, S.; Zhang, X., Explosives detection in a lasing plasmon nanocavity. *Nature Nanotechnology* **2014,** *9* (8), 600-604.

47. Wang, S.; Li, B.; Wang, X.-Y.; Chen, H.-Z.; Wang, Y.-L.; Zhang, X.-W.; Dai, L.; Ma, R.-M., High-Yield Plasmonic Nanolasers with Superior Stability for Sensing in Aqueous Solution. *ACS Photonics* **2017,** *4* (6), 1355-1360.

48. Sani, M.; Hosseini Farzad, M.; Hatef, A.; Safarzadeh, F., Tunable Anderson localization of propagating graphene surface plasmon modes in a random modulated graphene monolayer. *EPL (Europhysics Letters)* **2018,** *122* (6), 67004.

49. Sani, M.; Hosseini Farzad, M., Anderson localization of surface plasmons in monolayer graphene. *Physical Review B* **2018,** *97* (8), 085406.

50. Falkovsky, L. A., Optical properties of graphene. *Journal of Physics: Conference Series* **2008,** *129*, 012004.

51. Falkovsky, L. A.; Pershoguba, S. S., Optical far-infrared properties of a graphene monolayer and multilayer. *Physical Review B* **2007,** *76* (15), 153410.

52. Tao, J.; Yu, X.; Hu, B.; Dubrovkin, A.; Wang, Q. J., Graphene-based tunable plasmonic Bragg reflector with a broad bandwidth. *Optics Letters* **2014,** *39* (2), 271-274.

53. Lu, H.; Zeng, C.; Zhang, Q.; Liu, X.; Hossain, M. M.; Reineck, P.; Gu, M., Graphene-based active slow surface plasmon polaritons. *Scientific Reports* **2015,** *5*, 8443.

54. Wang, X.; Chen, C.; Pan, L.; Wang, J., A graphene-based Fabry-Pérot spectrometer in mid-infrared region. *Scientific Reports* **2016,** *6*, 32616.

55. Yan, H.; Low, T.; Zhu, W.; Wu, Y.; Freitag, M.; Li, X.; Guinea, F.; Avouris, P.; Xia, F., Damping pathways of mid-infrared plasmons in graphene nanostructures. *Nature Photonics* **2013,** *7*, 394.

56. Jayasekara, C.; Premaratne, M.; Stockman, M. I.; Gunapala, S. D., Multimode analysis of highly tunable, quantum cascade powered, circular graphene spaser. *Journal of Applied Physics* **2015,** *118* (17), 173101.

57. Chui, H. C.; Woods, G. L.; Fejer, M. M.; Martinet, E. L.; Jr., J. S. H., Tunable mid-infrared generation by difference frequency mixing of diode laser wavelengths in intersubband InGaAs/AlAs quantum wells. *Applied Physics Letters* **1995,** *66* (3), 265-267.

58. Galanzha, E. I.; Weingold, R.; Nedosekin, D. A.; Sarimollaoglu, M.; Nolan, J.; Harrington, W.; Kuchyanov, A. S.; Parkhomenko, R. G.; Watanabe, F.; Nima, Z.; Biris, A. S.; Plekhanov, A. I.; Stockman, M. I.; Zharov, V. P., Spaser as a biological probe. *Nature Communications* **2017,** *8* (1), 15528.

59. Song, P.; Wang, J.-H.; Zhang, M.; Yang, F.; Lu, H.-J.; Kang, B.; Xu, J.-J.; Chen, H.-Y., Three-level spaser for next-generation luminescent nanoprobe. *Science Advances* **2018,** *4* (8), eaat0292.